Journal of Statistical Physics, Vol. 89, Nos. 3/4, 1997

Product Measures and Dynamics for Solid-on-Solid Interfaces

Pierre Collet,[1] François Dunlop,[2] Damien P. Foster,[3] and Thierry Gobron[4]

Received August 23, 1996; final April 22, 1997

A two-species asymmetric exclusion process is considered with general transition rates subject only to the constraint of charge conservation. Conditions for the existence of a stationary product measure are found in both the cases of odd–even parallel dynamics and continuous-time dynamics. The results are then applied to a one-dimensional restricted solid-on-solid model, considered as a model of driven interfacial growth, showing a nontrivial dependence of the stationary measure on the external driving field. The dependence of the growth velocity on the slope of the interface is given and interface shapes in finite volume with opposite boundary conditions are investigated numerically.

KEY WORDS: R-SOS model; stochastic lattice gas; two-species exclusion process; odd–even dynamics.

1. INTRODUCTION

Asymmetric exclusion processes (one and two species) are of interest partly as they provide nontrivial realizations of systems out of equilibrium,[1] and because of the large number of models which may be simply mapped onto them. They are closely related to models of interfacial growth,[2] electrophoresis of polymers,[3] directed polymers in random media, and others.[4] A strong characterization of these models is obtained through a knowledge of their steady states. In certain cases these are obtained as

[1] Centre de Physique Théorique (CNRS-UPR14), Ecole Polytechnique, 91128 Palaiseau, France.

[2] Département de Physique, Université de Cergy-Pontoise, 95302 Cergy-Pontoise, France.

[3] Groupe de Physique Statistique (CNRS-EP127), Université de Cergy-Pontoise, 95302 Cergy-Pontoise, France.

[4] Laboratoire de Physique de la Matière Condensée (CNRS-URA D1254), Ecole Polytechnique, 91128 Palaiseau, France.

0022-4715/97/1100-0509$12.50/0

factorised probability measures.[5, 6, 7] Other steady states have been found using the Matrix Product Ansatz,[8, 9] which has been extended to two-species models[10] and sublattice parallel dynamics.[11, 12]

In the current article we consider a two-species model with charge conservation, more general than previously considered, and investigate the general conditions on the transition rates for the existence of a stationary product measure. The model is defined as follows. To each site of the lattice $\mathbb{Z}$ is associated a charge occupation number which may take on three values ($+1$, -1 and 0). This number may be interpreted as representing the state of a site: occupied by a positive or a negative particle, or empty. Allowed elementary transitions consist in a simultaneous change of the charge occupation numbers on two nearest-neighbor sites, conserving the total charge; each type of particle (positive or negative) is not, in general, conserved separately. The precise definition of the model is given in Section 2. Two different dynamics are considered:

1. An odd–even parallel dynamics: the bonds (i.e., the pairs of nearest-neighbor sites) are numbered in sequence. The odd-numbered bonds and the even-numbered bonds are updated alternately. One may think of updating the odd-numbered bonds just before half-integer times and the even-numbered bonds just before integer times.

2. A continuous time dynamics, which may be regarded as a time-rescaled limit of slow evolution of the odd–even dynamics, as will be seen in Section 3.

In both cases the dynamics is defined in terms of ten transition rates. We prove that there exists a codimension one manifold (i.e., nine dimensions) of dynamics with a one-parameter family of translationally invariant stationary product measures. The parameter is the charge density.

The results derived for the exclusion process are then applied to a restricted solid-on-solid (RSOS) model describing the growth of a stable phase at the expense of an unstable phase. In this mapping, bonds and sites are exchanged, and charge occupation numbers of the exclusion process become the height differences between neighboring sites in the growth model. A formal Hamiltonian is defined on the set of configurations of the RSOS model, depending on a parameter E, which may be identified to the difference of free energy density between the stable and the unstable phases the interface separates. The rates of elementary transitions are then chosen to satisfy a local detailed balance with respect to the formal Hamiltonian. In the case of odd–even dynamics, local detailed balance is not satisfied for a complete odd–even update, because the dynamics depends on the order in which one updates odd and even sites (even at $E=0$, where the

Gibbs measure associated with the Hamiltonian is invariant). For a non zero value of E, the usual Gibbs ansatz would not lead to a translation invariant stationary state. A notable feature of the stationary product measures found here is their non-trivial dependence upon the parameter E.

Using the invariant product measures, we compute the mean velocity of the interface as a function of the slope. For two fixed asymptotic slopes with distinct values, a concave or convex profile develops whose shape can be discussed in terms of a Wulff construction (see e.g., ref. 2 and bibliography therein), and dynamical phase transitions related to the occurrence of inflection points.

In finite volume, with slope fixing stochastic boundary conditions, the speed of translationally invariant states is given by the same function of the slope as in infinite volume. In the case of equal left and right boundary conditions, there is convergence to the product measure exactly computed. Numerical simulations allow us to look for stationary states in the case of boundary conditions which fix opposite slopes. Various stationary shapes are observed depending on temperature and driving field.

The paper is organized as follows: in Section 2 the exact solution for the product stationary measures in the case of odd–even dynamics is given; in Section 3 we present the results in the case of the continuous time dynamics. Section 4 is devoted to the interface dynamics, including local detailed balance, in both the odd–even and continuous time dynamics. The interface velocity is discussed in Section 5. Section 6 concerns the finite volume states of uniform average slope and numerical results for inhomogeneous interfaces in finite volume are given in Section 7.

2. ODD–EVEN DYNAMICS FOR A TWO SPECIES EXCLUSION MODEL

In this section we define the discrete time dynamics for our system in terms of a two species particle system on a one dimensional lattice. A given site can be either empty or occupied by at most one particle of positive or negative charge, so that we associate each configuration with a sequence in $\{-1, 0, 1\}^{\mathbb{Z}}$. We implement an "odd–even" dynamics in the following way: we first define a local transition operator T_i, whose action on the cylindrical functions depends only on the charge occupation numbers on sites $i-1$ and i in a given configuration $\mathbf{x}$:

$$T_i f(\mathbf{x}) = f(\mathbf{x}) + \sum_{\alpha,\beta=-1}^{1} \chi_i^{\alpha,\beta}(\mathbf{x}) \sum_{k \in K_{\alpha,\beta}} C^k_{\alpha,\beta}(f(S_i^k \mathbf{x}) - f(\mathbf{x})) \qquad (2.1)$$

where $\chi_i^{\alpha,\beta}$ is the indicatrix of the local configuration:

$$\chi_i^{\alpha,\beta}(\mathbf{x}) = \begin{cases} 1 & \text{if } x_{i-1}=\alpha \quad \text{and} \quad x_i=\beta; \\ 0 & \text{otherwise} \end{cases} \tag{2.2}$$

$K_{\alpha,\beta}$ is the set of allowed changes when those occupation numbers are precisely α, β:

$$K_{\alpha,\beta} = \{k \neq 0 \text{ such that } |\alpha+k| \leqslant 1 \text{ and } |\beta-k| \leqslant 1\} \tag{2.3}$$

S_i^k is an operator which increases by k the charge at site $i-1$ when permitted and correspondingly decreases the charge at site i by the same amount so that the total charge is conserved:

$$(S_i^k \mathbf{x})_j = \begin{cases} x_{i-1}+k & \text{if } j=i-1 \quad \text{and} \quad k \in K_{x_{i-1},x_i}; \\ x_i-k & \text{if } j=i \quad \text{and} \quad k \in K_{x_{i-1},x_i}; \\ x_j & \text{otherwise} \end{cases} \tag{2.4}$$

Particle exclusion and charge conservation restrict the number of possible transitions to five pairs, corresponding respectively to the creation of particles of opposite charges, annihilation, exchange, or propagation of + or − charges in either direction. The corresponding rates $C_{\alpha,\beta}^k$ can be adjusted freely provided the total coefficient of $f(\mathbf{x})$ in (2.1) remains positive (T_i must be positivity preserving):

$$\sum_{k \in K_{\alpha,\beta}} C_{\alpha,\beta}^k \leqslant 1 \quad \forall \alpha, \beta \tag{2.5}$$

Now taking into account the fact that any two local transition operators T_i and T_j commute provided $|i-j| \neq 1$, we can define without ambiguity two transition operators T^{odd} and T^{even} as the product of local transition operators acting on odd and even pairs of neighboring sites respectively:

$$T^{\text{odd}} = \prod_i T_{2i-1} \tag{2.6}$$

and

$$T^{\text{even}} = \prod_i T_{2i} \tag{2.7}$$

Finally we implement the "odd–even" dynamics per unit time by defining an evolution operator L acting on cylindrical functions:

$$(Lf)(\mathbf{x}) = (T^{\text{odd}} T^{\text{even}} f)(\mathbf{x}) \tag{2.8}$$

The evolution over an arbitrary integer time t is then given by the operator L^t. Separately, T^{odd} or T^{even} may be taken as the evolution operators over half-integer times.

We now look for stationary product measures for this model. In view of the structure of the evolution operator, stationary product measures can be looked for of the form:

$$\mu(\mathbf{x}) = \prod_i Q(x_{2i})\, R(x_{2i+1}) \tag{2.9}$$

where Q, R are two different measures on the set $\{-1, 0, 1\}$.

Due to the translational invariance of Eqs. (2.8) and (2.9), the stationarity equations,

$$\mu(\mathbf{x}) = (\mu T^{\text{odd}} T^{\text{even}})(\mathbf{x}) \tag{2.10}$$

can be solved locally:

$$(Q \otimes R)(x_0, x_1) = ((R \otimes Q) T_1)(x_0, x_1) \tag{2.11}$$

Using (2.1), we obtain for all α, β in $\{-1, 0, 1\}$:

$$\begin{aligned} Q(\alpha)\, R(\beta) = R(\alpha)\, Q(\beta) \\ + \sum_{k \in K_{\alpha,\beta}} (C^{-k}_{\alpha+k,\beta-k} R(\alpha+k)\, Q(\beta-k) - C^{k}_{\alpha,\beta} R(\alpha)\, Q(\beta)) \end{aligned} \tag{2.12}$$

This system of nine equations can be partitioned according to the five possible values of the conserved quantity $\alpha + \beta$. Normalization of transition probabilities reduces the number of equations by one for each value of $\alpha + \beta$. This results in a set of four independent homogeneous equations:

$$\begin{aligned} (1 - C^{-1}_{0,-1})\, Q(-1)\, R(0) &= (1 - C^{1}_{-1,0})\, Q(0)\, R(-1) \\ (1 - C^{1}_{0,1})\, Q(1)\, R(0) &= (1 - C^{-1}_{1,0})\, Q(0)\, R(1) \\ C^{-1}_{0,0} Q(0)\, R(0) &= (1 - C^{-2}_{1,-1})\, Q(-1)\, R(1) \\ &\quad - (1 - C^{1}_{-1,1} - C^{2}_{-1,1})\, Q(1)\, R(-1) \\ C^{1}_{0,0} Q(0)\, R(0) &= (1 - C^{2}_{-1,1})\, Q(1)\, R(-1) \\ &\quad - (1 - C^{-1}_{1,-1} - C^{-2}_{1,-1})\, Q(-1)\, R(1) \end{aligned} \tag{2.13}$$

We now assume $C^{\pm 1}_{0,\pm 1} < 1$, $C^{\mp 1}_{\pm 1,0} < 1$, which leaves aside totally asymmetric models, and then also assume $R(0) > 0$, $Q(0) > 0$, which leaves aside one-species models. The first two equations in (2.13) then allow us to define an unknown $c > 0$ by

$$c^2 = \frac{Q(1)\,Q(-1)}{(1-C^1_{-1,0})(1-C^{-1}_{1,0})\,Q(0)^2} = \frac{R(1)\,R(-1)}{(1-C^{-1}_{0,-1})(1-C^1_{0,1})\,R(0)^2} \tag{2.14}$$

The last two equations in (2.13) can then be written with c as the only unknown, and their compatibility is the only condition for existence of solutions.

In the case when particles are conserved, $C^{\pm 1}_{0,0} = 0$, $C^{-1}_{1,-1} = 0$, $C^1_{-1,1} = 0$, the last two equations in (2.13) are compatible if and only if

$$(1-C^{-2}_{1,-1})(1-C^1_{-1,0})(1-C^1_{0,1}) = (1-C^2_{-1,1})(1-C^{-1}_{0,-1})(1-C^{-1}_{1,0}) \tag{2.15}$$

and any value of c is allowed.

In the general case when $C^1_{0,0} + C^{-1}_{0,0} > 0$, the last two equations in (2.13) are compatible if and only if

$$\frac{(1-C^{-2}_{1,-1})(C^1_{0,0}+C^{-1}_{0,0}) - C^{-1}_{0,0}C^{-1}_{1,-1}}{(1-C^{-1}_{0,-1})(1-C^{-1}_{1,0})} = \frac{(1-C^2_{-}1,1)(C^1_{0,0}+C^{-1}_{0,0}) - C^1_{0,0}C^1_{-1,1}}{(1-C^1_{-1,0})(1-C^1_{0,1})} \tag{2.16}$$

and c is the positive root of

$$c^2 = \frac{C^1_{0,0}+C^{-1}_{0,0}}{C^{-1}_{1,-1}(1-C^1_{0,1})(1-C^1_{-1,0}) + C^1_{-1,1}(1-C^{-1}_{0,-1})(1-C^{-1}_{1,0})} \tag{2.17}$$

Having determined c, or chosen c in the case of particle conservation, the ratios $R(1)\,R(-1)/R(0)^2$ and $Q(1)\,Q(-1)/Q(0)^2$ are fixed; there remains a free parameter which may be defined by

$$y^2 = \frac{(1-C^{-1}_{0,-1})\,R(1)}{(1-C^1_{0,1})\,R(-1)} = \frac{(1-C^1_{-1,0})\,Q(1)}{(1-C^{-1}_{1,0})\,Q(-1)}$$

This allows us to write down explicitly the solutions to (2.12) as a one-parameter (non-conserved case) or two-parameter (conserved case) family of stationary product measures:

$$
\begin{aligned}
Q(1) &= \frac{c(1-C^{-1}_{1,0})\,y}{1+c(1-C^{-1}_{1,0})\,y+c(1-C^{1}_{-1,0})\,y^{-1}} \\
Q(0) &= \frac{1}{1+c(1-C^{-1}_{1,0})\,y+c(1-C^{1}_{-1,0})\,y^{-1}} \\
Q(-1) &= \frac{c(1-C^{1}_{-1,0})\,y^{-1}}{1+c(1-C^{-1}_{1,0})\,y+c(1-C^{1}_{-1,0})\,y^{-1}} \\
R(1) &= \frac{c(1-C^{1}_{0,1})\,y}{1+c(1-C^{1}_{0,1})\,y+c(1-C^{-1}_{0,-1})\,y^{-1}} \\
R(0) &= \frac{1}{1+c(1-C^{1}_{0,1})\,y+c(1-C^{-1}_{0,-1})\,y^{-1}} \\
R(-1) &= \frac{c(1-C^{-1}_{0,-1})\,y^{-1}}{1+c(1-C^{1}_{0,1})\,y+c(1-C^{-1}_{0,-1})\,y^{-1}}
\end{aligned}
\tag{2.18}
$$

The parameter y is related to the charge density of the system, which we denote ρ, through the following formula:

$$
\rho = \tfrac{1}{2} \sum_{x=-1}^{1} x(Q(x)+R(x)) \tag{2.19}
$$

In the conserved case, the other free parameter c fixes the particle density. The charge density ρ is a strictly monotonous function of y from $]0, +\infty[$ onto $]-1, 1[$, for all values of the jump rates.

Another quantity of interest is the average current J across the system for these invariant measures:

$$
J = -\sum_{\alpha,\beta=-1}^{1} \sum_{k\in K_{\alpha,\beta}} kC^{k}_{\alpha,\beta} R(\alpha)\,Q(\beta) = \sum_{x=-1}^{1} x(R(x)-Q(x)) \tag{2.20}
$$

where the second expression is deduced from the first using the stationarity equations (2.12).

3. CONTINUOUS DYNAMICS

Another possible way of defining a dynamics in such models is to consider a continuous time process. We now define a local infinitesimal generator by

$$
L_i f(\mathbf{x}) = \sum_{\alpha,\beta=-1}^{1} \chi_i^{\alpha,\beta}(\mathbf{x}) \sum_{k\in K_{\alpha,\beta}} \Gamma^{k}_{\alpha,\beta}(f(S_i^k\mathbf{x})-f(\mathbf{x})) \tag{3.1}
$$

together with (2.2–2.4) and the evolution on the space of cylindrical functions as

$$\frac{\partial f}{\partial t}(\mathbf{x}) = \frac{1}{\tau}\sum_i (L_i f)(\mathbf{x}) \tag{3.2}$$

where $\tau > 0$ fixes the time scale: A simple correspondence can be found between continuous and odd–even dynamics, since the discrete time evolution generator defined through (2.8) converges weakly to that of (3.2), when both time scale and jump rates are rescaled by a factor ε, as

$$C^k_{\alpha,\beta} = \frac{\varepsilon}{\tau} \Gamma^k_{\alpha,\beta} \tag{3.3}$$

in the limit when ε goes to zero. Correlatively, one may investigate the condition of existence of stationary product measures associated to (3.1). It is the same as the one obtained through an expansion in ε of relation (2.15) or (2.16) to the first non trivial (second) order:

$$\Gamma^2_{-1,1} - \Gamma^{-2}_{1,-1} = (\Gamma^1_{0,1} - \Gamma^{-1}_{1,0}) + (\Gamma^1_{-1,0} - \Gamma^{-1}_{0,-1}) \qquad \text{(conserved case)} \tag{3.4}$$

or

$$\Gamma^2_{-1,1} - \Gamma^{-2}_{1,-1} + \frac{\Gamma^1_{-1,1}\Gamma^1_{0,0} - \Gamma^{-1}_{1,-1}\Gamma^{-1}_{0,0}}{\Gamma^1_{0,0} + \Gamma^{-1}_{0,0}}$$
$$= (\Gamma^1_{0,1} - \Gamma^{-1}_{1,0}) + (\Gamma^1_{-1,0} - \Gamma^{-1}_{0,-1}) \qquad \text{(non-conserved case)} \tag{3.5}$$

In this case there is no difference between sublattices, and there is a one parameter family of stationary product measures μ which can be written as:

$$\mu(\mathbf{x}) = \prod_i P(x_i)$$

with

$$P(1) = \frac{cy}{1 + cy + cy^{-1}}$$
$$P(0) = \frac{1}{1 + cy + cy^{-1}} \tag{3.6}$$
$$P(-1) = \frac{cy^{-1}}{1 + cy + cy^{-1}}$$

where the parameter $y>0$ has the same significance as previously, and is related to the charge density ρ, as

$$\rho=\frac{c(y-y^{-1})}{1+cy+cy^{-1}} \tag{3.7}$$

In the conserved particles case, c is arbitrary and fixes the particle density; in the nonconserved case c is the positive root of

$$c^2=\frac{\Gamma^1_{0,0}+\Gamma^{-1}_{0,0}}{\Gamma^{-1}_{1,-1}+\Gamma^1_{-1,1}} \tag{3.8}$$

The last three equations can be also be recovered from equations (2.17–2.19) in the limit $\varepsilon\to 0$.

4. INTERFACE DYNAMICS WITH LOCAL DETAILED BALANCE

As is well known, the exclusion model of the previous sections can be mapped onto a problem of restricted solid-on-solid interface dynamics. In this setting each configuration of the interface is associated to a sequence of integers, $\mathbf{h}=\{h_i\}_{i\in\mathbb{Z}}$, $h_i\in\mathbb{Z}$, which represent the vertical location of the interface at site i—*the heights*. Furthermore, the configurations are restricted to those in which the height differences between neighboring sites differ by at most one unit:

$$|h_{i+1}-h_i|\leqslant 1\ \forall i\in\mathbb{Z} \tag{4.1}$$

so that the previously defined charge occupation number at site i, can be taken as the height difference between sites i and $i+1$:

$$x_i=h_{i+1}-h_i \qquad \text{for all} \quad i\in\mathbb{Z} \tag{4.2}$$

As a consequence of the conservation of charge, Eq. (2.8) defines also a local dynamics for the height variables $\mathbf{h}$.

In this setting, we introduce the following formal Hamiltonian:

$$H(\mathbf{h})=\sum_{i=-\infty}^{+\infty} J\,|h_{i+1}-h_i|-E\sum_{i=-\infty}^{+\infty} h_i \tag{4.3}$$

where J and E are both positive constants, and choose the rates $C^k_{\alpha,\beta}$ so that T_i as defined in (2.1) obeys the detailed balance rules with respect

to H. This dynamics was previously considered in ref. 13. All transitions which increment by k the ith height require:

$$\frac{C^{k}_{h_i-h_{i-1},\,h_{i+1}-h_i}}{C^{-k}_{h_i-h_{i-1}+k,\,h_{i+1}-h_i-k}} = \exp\left(-\frac{1}{kT}\left(H(S_i^k\mathbf{h})-H(\mathbf{h})\right)\right) \tag{4.4}$$

The use of the notation S_i^k in the right hand side of Eq. (4.4) is justified by the fact that any local difference depends only on the x variables. The above equations amount to writing the ten jump rates $C^k_{\alpha,\beta}$ in terms of five positive parameters $v_\gamma, \gamma \in \{0, \pm 1, \pm 2\}$:

$$C^k_{\alpha,\beta} = e^{-\Delta H/2kT} v_{3\alpha+\beta+k} = b^{|k|-|\alpha|-|\beta|} a^{-k} v_{3\alpha+\beta+k} \tag{4.5}$$

where we have introduced

$$a = \exp\left\{-\frac{E}{2kT}\right\} \qquad b = \exp\left\{-\frac{J}{kT}\right\} \tag{4.6}$$

and

$$\Delta H = H(S_i^k\mathbf{h}) - H(\mathbf{h})$$

The five pairs of allowed transitions are represented in Fig. 1.

The v_γ can be adjusted freely. The positivity preserving relations (2.5) now reads

$$\begin{aligned} &v_2 \leqslant a, \qquad v_{-2} \leqslant a, \qquad a^{-1}v_1 + a v_{-1} \leqslant b^{-1} \\ &b^{-1}a^{-1}v_{-1} + a^{-2}v_0 \leqslant 1, \qquad b^{-1}a v_1 + a^2 v_0 \leqslant 1 \end{aligned} \tag{4.7}$$

Imposing left-right symmetry in tile transitions would require $v_2 = v_{-2}$. In this case there are four different transition channels. $\Delta H = \pm E, \pm 2E$,

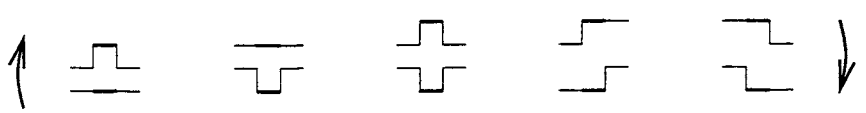

$C^1_{0,0}=ba^{-1}v_1$ $C^1_{-1,1}=b^{-1}a^{-1}v_{-1}$ $C^2_{-1,1}=a^{-2}v_0$ $C^1_{0,1}=a^{-1}v_2$ $C^1_{-1,0}=a^{-1}v_{-2}$
$C^{-1}_{1,-1}=b^{-1}av_1$ $C^{-1}_{0,0}=bav_{-1}$ $C^{-2}_{1,-1}=a^2v_0$ $C^{-1}_{1,0}=av_2$ $C^{-1}_{0,-1}=av_{-2}$

Fig. 1. Representation of allowed transitions, and corresponding rates: the first line gives the rates in the direction of the up arrow, and the second line the rates in the direction of the down arrow.

$\pm(2J-E)$, $\pm(2J+E)$. When $|\Delta H|$ takes four distinct values, Eq. (4.5) could be rewritten as

$$C^k_{\alpha,\beta} = \Phi(\Delta H)$$

with an arbitrary positive function Φ satisfying[1]

$$\Phi(-\Delta H) = e^{\Delta H/kT}\Phi(\Delta H)$$

Using the formulation of detailed balance (4.5), the condition of existence of a product measure (2.16)–(2.17) for the height differences becomes:

$$v_0 = \frac{v_2 + v_{-2} - v_2 v_{-2}(a^{-1}+a)}{a + a^{-1} - v_2 - v_{-2}} \qquad \text{(conserved case: } v_1 = v_{-1} = 0\text{)}, \quad (4.8)$$

or

$$v_0 + \frac{v_1 v_{-1} b^{-1}}{v_{-1} a + v_1 a^{-1}} = \frac{v_2 + v_{-2} - v_2 v_{-2}(a^{-1}+a)}{a + a^{-1} - v_2 - v_{-2}}$$

$$\text{(non-conserved case: } v_1 + v_{-1} > 0\text{)} \qquad (4.9)$$

For any value of a and b, there always exist a dynamics which simultaneously satisfy the restrictions (4.7) and (4.8) or (4.9).

The one-parameter family of stationary product measures now read

$$\begin{aligned}
Q(1) &= \frac{c(1-av_2)\,y}{1 + c(1-av_2)\,y + c(1-a^{-1}v_{-2})\,y^{-1}} \\
Q(0) &= \frac{1}{1 + c(1-av_2)\,y + c(1-a^{-1}v_{-2})\,y^{-1}} \\
Q(-1) &= \frac{c(1-a^{-1}v_{-2})\,y^{-1}}{1 + c(1-av_2)\,y + c(1-a^{-1}v_{-2})\,y^{-1}} \\
R(1) &= \frac{c(1-a^{-1}v_2)\,y}{1 + c(1-a^{-1}v_2)\,y + c(1-av_{-2})\,y^{-1}} \\
R(0) &= \frac{1}{1 + c(1-a^{-1}v_2)\,y + c(1-av_{-2})\,y^{-1}} \\
R(-1) &= \frac{c(1-av_{-2})\,y^{-1}}{1 + c(1-a^{-1}v_2)\,y + c(1-av_{-2})\,y^{-1}}
\end{aligned} \qquad (4.10)$$

where the parameter c is arbitrary in the conserved case, and otherwise is the positive root of

$$c^2 = \frac{b^2(a^{-1}v_1 + av_{-1})}{av_1(1-a^{-1}v_2)(1-a^{-1}v_{-2}) + a^{-1}v_{-1}(1-av_2)(1-av_{-2})} \tag{4.11}$$

The stationary measures depend in a non trivial way on the external driving field E through the parameter a, even when left right symmetry is imposed ($v_2 = v_{-2}$).

The auxiliary parameter y is now related to the mean slope of the interface, which we denote $\tan\theta$, through the following formula:

$$\begin{aligned}\tan\theta &= \frac{1}{2}\sum_{x=-1}^{1} x(Q(x)+R(x)) \\ &= \frac{cy(1-av_2) - cy^{-1}(1-a^{-1}v_{-2})}{2(1+cy(1-av_2)+cy^{-1}(1-a^{-1}v_{-2}))} \\ &\quad + \frac{cy(1-a^{-1}v_2) - cy^{-1}(1-av_{-2})}{2(1+cy(1-a^{-1}v_2)+cy^{-1}(1-av_{-2}))}\end{aligned} \tag{4.12}$$

We now give some explicit examples of the product measure for different realizations of the dynamics.

4.1. Heat Bath Dynamics

A simple case is provided by thermal bath dynamics, where independence of the transition probabilities from the incoming state fixes the amplitudes in all channels:

$$\begin{aligned} v_{-2} = v_2 &= \frac{1}{a^{-1}+a} \\ v_0 &= \frac{b^2}{1+a^{-2}b^2+a^2b^2} \\ v_1 &= \frac{a^{-1}b}{1+a^{-2}b^2+a^2b^2} \\ v_{-1} &= \frac{ab}{1+a^{-2}b^2+a^2b^2} \end{aligned} \tag{4.13}$$

In this case, relation (4.9) is found to be satisfied. The constant c is given by:

$$c = b(a+a^{-1}) \tag{4.14}$$

and the stationary product measures now reads

$$\begin{aligned} Q(1) &= \frac{y^2}{y^2 + yab^{-1} + a^2} & R(1) &= \frac{y^2a^2}{y^2a^2 + yab^{-1} + 1} \\ Q(0) &= \frac{yab^{-1}}{y^2 + yab^{-1} + a^2} & R(0) &= \frac{yab^{-1}}{y^2a^2 + yab^{-1} + 1} \\ Q(-1) &= \frac{a^2}{y^2 + yab^{-1} + a^2} & R(-1) &= \frac{1}{y^2a^2 + yab^{-1} + 1} \end{aligned} \tag{4.15}$$

where the auxiliary parameter y is related to the average slope $\tan\theta$, through:

$$2\tan\theta = \sum_{x=-1}^{1} x(Q(x) + R(x)) = \frac{y^2 - a^2}{y^2 + yab^{-1} + a^2} + \frac{y^2a^2 - 1}{y^2a^2 + yab^{-1} + 1} \tag{4.16}$$

4.2. Metropolis Dynamics

A Metropolis dynamics for the RSOS model is defined as follows:

(i) attempt rates w_1 and w_2 corresponding respectively to $k = \pm 1$ and $k = \pm 2$, are fixed independently of the Hamiltonian (this will not in general be compatible with an invariant product measure);

(ii) The transition rates are taken as

$$C^k_{\alpha,\beta} = \begin{cases} \exp\{-\Delta H_+(\alpha, \beta; k)\}\ w_{|k|} & \text{if } |\alpha + k| \leqslant 1 \text{ and } |\beta - k| \leqslant 1 \\ 0 & \text{otherwise} \end{cases} \tag{4.17}$$

with

$$\Delta H_+(\alpha, \beta; k) = \max\{J|\alpha + k| + |\beta - k| - Ek - J|\alpha| - J|\beta|, 0\} \tag{4.18}$$

The correspondence with the v_γ is given by:

$$\begin{aligned} &v_2 = v_{-2} = aw_1, \qquad v_0 = a^2w_2, \qquad v_{-1} = baw_1 \\ &v_1 = \begin{cases} ba^{-1}w_1 & \text{if } E \leqslant 2J \quad (\text{i.e. } a \geqslant b) \\ b^{-1}aw_1 & \text{if } E \geqslant 2J \quad (\text{i.e. } a \leqslant b) \end{cases} \end{aligned} \tag{4.19}$$

Assuming for definiteness $a \geqslant b$, we find from (4.19) the necessary relation between w_1 and w_2 in order to get an invariant product measure:

$$a^2w_2 + \frac{w_1}{a^{-2} + a^2} = aw_1 \frac{2 - a(a^{-1} + a)\, w_1}{a^{-1} + a - 2aw_1} \tag{4.20}$$

The restriction $w_1 \leqslant 1/2$ is sufficient to satisfy the inequalities (4.7). The requirement $w_2 \geqslant 0$ is always fulfilled when $w_1 \geqslant 0$. There is thus a one-parameter family of Metropolis dynamics with invariant product measures given by (4.10), which take the form:

$$\begin{aligned} Q(1) &= \frac{c(1-a^2 w_1)\, y}{d_Q} \qquad Q(0) = \frac{1}{d_Q} \qquad Q(-1) = \frac{c(1-w_1)\, y^{-1}}{d_Q} \\ R(1) &= \frac{c(1-w_1)\, y}{d_R} \qquad R(0) = \frac{1}{d_R} \qquad R(-1) = \frac{c(1-a^2 w_1)\, y^{-1}}{d_R} \end{aligned} \tag{4.21}$$

$$\begin{aligned} d_Q &= 1 + c(1-a^2 w_1)\, y + c(1-w_1)\, y^{-1} \\ d_R &= 1 + c(1-w_1)\, y + c(1-a^2 w_1)\, y^{-1} \end{aligned} \tag{4.22}$$

$$c^2 = \frac{b^2(a^{-2}+a^2)}{(1-w_1)^2 + (1-a^2 w_1)^2}$$

4.3. Continuous Time Dynamics

The setting is as in Section 3, with (3.3) becoming

$$v_y = \frac{\varepsilon}{\tau} u_y \tag{4.23}$$

In the limit $\varepsilon \searrow 0$, a continuous dynamics is obtained, and the condition for an invariant product measure becomes

$$u_0 = \frac{u_2 + u_{-2}}{a^{-1} + a} \qquad \text{(conserved case: } u_1 = u_{-1} = 0) \tag{4.24}$$

or

$$u_0 + \frac{u_1 u_{-1} b^{-1}}{u_{-1} a + u_1 a^{-1}} = \frac{u_2 + u_{-2}}{a + a^{-1}}$$

$$\text{(non-conserved case: } u_1 + u_{-1} > 0) \tag{4.25}$$

The invariant measure is of the form (3.6). In the conserved particles case, c is arbitrary; in the non-conserved case c is the positive root of

$$c^2 = b^2 \frac{a^{-1} u_1 + a u_{-1}}{a u_1 + a^{-1} u_{-1}} \tag{4.26}$$

The invariant measure depends upon E except when $u_{-1} = u_1$.

5. SPEED OF THE INTERFACE IN AN INVARIANT MEASURE

The mean velocity of the interface does not depend on the absolute height of the interface and can therefore be computed using the measure for the height differences. It is equal to minus the average current defined in Section 2 and its expression for any product measure reads:

$$V = \langle h_i(t+1) - h_i(t) \rangle = \sum_{\alpha,\beta=-1}^{1} \sum_{k \in K_{\alpha,\beta}} k C^k_{\alpha,\beta} R(\alpha)\, Q(\beta) \tag{5.1}$$

Using the stationarity Eqs. (2.12), one can transform the quadratic Eq. (5.1) into a linear one:

$$\begin{aligned} V &= \sum_{x=-1}^{1} x(Q(x) - R(x)) \\ &= \frac{c(a^{-1}-a)(2c[v_2 + v_{-2} - (a^{-1}+a)\, v_2 v_{-2}] + v_2 y + v_{-2} y^{-1})}{\begin{pmatrix} ((1+cy(1-av_2) + cy^{-1}(1-a^{-1}v_{-2})) \\ \times (1+cy(1-a^{-1}v_2) + cy^{-1}(1-av_{-2})) \end{pmatrix}} \end{aligned} \tag{5.2}$$

In the case when left-right symmetry is imposed, $v_{-2} = v_2$, the velocity becomes an even function of the average slope $\tan\theta$ (cf. (4.12)). It is then sufficient to discuss $\tan\theta \geqslant 0$. At $\tan\theta = 0$, the first derivative of V with respect to $\tan\theta$ is of course $V'(0) = 0$, and the sign of the second derivative $V''(0)$ is the same as that of the first derivative of V with respect to $z = (y + y^{-1})/2$ at $z = 1$. We thus find, up to positive factors,

$$V''(0) \approx 1 - c(1 - a^{-1}v_2) - c(1 - av_2) - 8c^2(1 - a^{-1}v_2)(1 - av_2) \tag{5.3}$$

We also need

$$V''(1) \approx 2(1 - a^{-1}v_2)(1 - av_2)\, c^2 - 1 \tag{5.4}$$

For the heat bath algorithm, Eqs. (5.3)–(5.4) simplify to

$$V''(0) \approx 1 - ba^{-1} - ba - 8b^2 \tag{5.5}$$

$$V''(1) \approx 2b^2 - 1 \tag{5.6}$$

Convex or concave profiles on the infinite line can be stable or unstable depending on whether $V(\tan\theta)$ coincides with its concave or convex envelope over the interval between the asymptotic conditions at $\pm\infty$.[2] Taking the number and type of possible invariant shapes as a

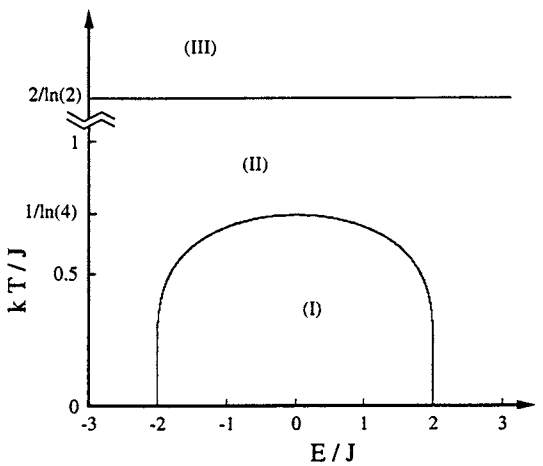

Fig. 2. Phase diagram in the case of heat-bath dynamics: in region (I), the velocity V is maximum for a non zero slope and admits an inflexion point between zero and the position of the maximum; in regions (II) and (III), the velocity is maximum for zero slope; in region (III) the velocity admits an inflexion point near $\tan\theta = 1$.

dynamical order parameter, transition lines are given by $V''(0) = 0$ and $V''(1) = 0$, as shown in Fig. 2.

Another interesting quantity is the mobility or linear response coefficient for the speed as function of the field. It is here the sum of the contributions from the dependence of both the measure and the rates on the external field. For $v_{-2} = v_2$, it reads

$$\frac{1}{\beta} \lim_{E \searrow 0} \frac{V}{E} = \frac{bv_2}{1 - v_2} \frac{4b + y + y^{-1}}{(1 + b(y + y^{-1}))^2} \tag{5.7}$$

In the case of the thermal bath, both dependences contribute equally.

6. UNIFORM INVARIANT MEASURES FOR FINITE SYSTEMS

In finite volume we consider sequences, $\{h_i\}_{i \in [-2, L, 2L]}$, with some boundary conditions. The position of the interface is, to some extent, arbitrary, and may be fixed by, say, setting $h_{-2L} = 0$, leaving $4L$ independent variables. We choose to update the odd sites just before half-integer times and the even sites just before integer times.

Here we consider two possible specifications of the boundary conditions for which the odd-even uniform product measure (4.10) plays an important role. It is convenient to specify these boundary conditions in terms of the height differences $x_i = h_{i+1} - h_i$, defined for $i \in [-2L, 2L - 1]$.

6.1. Slope Fixing Stochastic Boundary Conditions

We consider a lattice with open boundary conditions. Updating h_i is equivalent to considering all the possible transitions for the pair (x_{i-1}, x_i). For odd-site updates, all the x_i are naturally considered in pairs, implying that T^{odd} may be defined as before (Eq. (2.6)). For the even-site updates x_{-2L} and x_{2L-1} cannot be paired, and their update needs be specified through a modification of T^{even}. A natural choice is to update the unpaired sites stochastically. If x_{-2L} is chosen according to the distribution $R(x)$ and x_{2L-1} according to the distribution $Q(x)$, for a given choice of y, the measure

$$\mu_{\text{stoch}}(\mathbf{x}) = R(x_{-2L}) \left(\prod_{i=-L+1}^{L-1} Q(x_{2i-1})\, R(x_{2i}) \right) Q(x_{2L-1}) \tag{6.1}$$

is invariant under evolution of integer times.

While all the equal time correlation functions will remain the same as in the infinite system, the two-time correlations will differ, reflecting the different update scheme at the boundaries with respect to the bulk. With these boundary conditions the total height difference $h_{2L} - h_{-2L}$ is no longer conserved, and the slope of the interface is only given as an average quantity, whose value is the same as in the infinite volume limit.

A modified form of these stochastic boundary conditions will be used in the following section to generate non-uniform interface profiles. There the stochastic update of the boundary sites is done with $R_{\theta_1}(x)$ for $i = -2L$ and $Q_{\theta_2}(x)$ for $i = 2L-1$, where $\tanh(\theta_1)$ and $\tanh(\theta_2)$ are the slopes of the interfaces in the respective uniform cases.

6.2. Tilted Periodic Boundary Conditions

Periodic boundary conditions are implemented in the space of the height differences x_i by identifying $x_{2L} = x_{-2L}$. The conservation of charge

$$\sum_{i=-2L}^{2L-1} x_i = h_{2L} - h_{-2L} \tag{6.2}$$

adds an additional constraint to the evolution of the system. The measure, invariant under integer time evolution, takes the form:

$$\mu_{\text{periodic}}(\mathbf{x}) = \left(\prod_{i=-L+1}^{L-1} Q(x_{2i-1})\, R(x_{2i}) \right) Q(x_{2L-1})\, R(x_{-2L}) \times \delta\left(\sum_{i=-2L}^{2L-1} x_i - 4L \tan\theta \right) \tag{6.3}$$

were the tilt of the interface, θ, has been defined through

$$h_{2L} - h_{-2L} = 4L \tan \theta \tag{6.4}$$

Since the x take only integer values, $4L \tan \theta$ must be integer. While the measure (6.3) remains invariant with these boundary conditions, it is of interest to know if it is generically selected. Figure 3 shows the velocity-

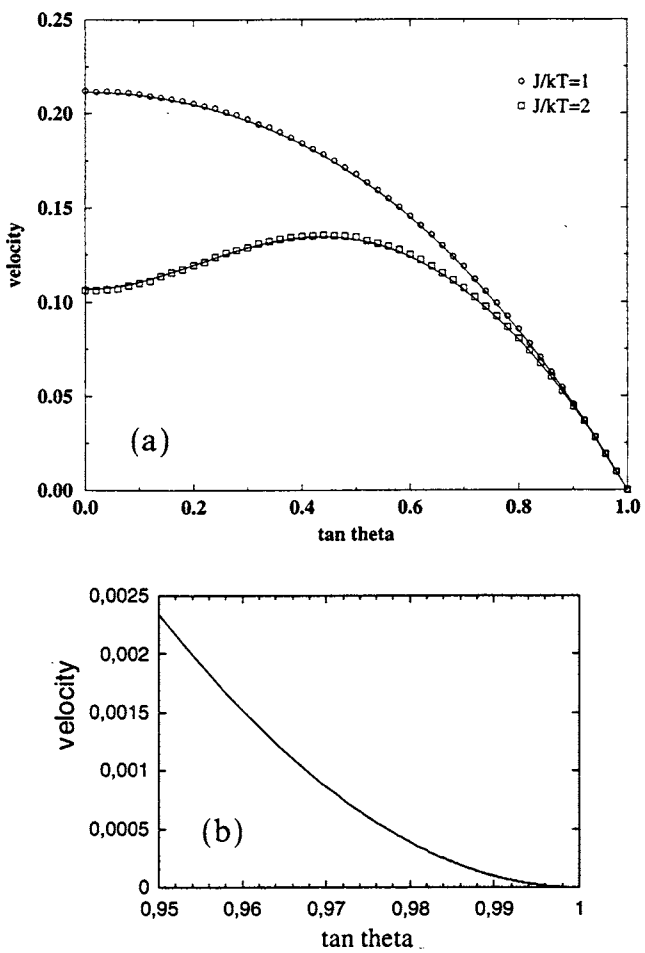

Fig. 3. (a) Plot of the velocity as a function of the slope for two sets of parameters: (I) $E/kT = 0.5$, $J/kT = 1$ and (II) $E/kT = 0.5$, $J/kT = 2$. Solid lines represent the analytic results, and the circles and squares Monte Carlo results for a system of size $N = 100$ and periodic boundary conditions. (b) Plot of the velocity as a function of the slope for $a = \exp(-E/2kT) = 0.99$, $b = \exp(-J/kT) = 0.99$, corresponding to region (III) of Fig. 2 (analytical).

angle plots for various values of the model parameters and heat-bath dynamics, compared with the expression (5.2) which is exact in the infinite volume limit. Starting from a state were all the $x_i = 0$, the finite system evolved towards the stationary state (6.3). Other initial conditions were also taken, and in each case the system evolved towards the results predicted by the product measure for the infinite systems, up to corrections of $O(1/L)$ caused by the additional constraint on the slope.

7. INTERFACE SHAPES IN FINITE VOLUME: NUMERICAL RESULTS

In this section we investigate the behavior of non-homogeneous interfaces in finite systems, and in particular the existence of so-called roof-shaped profiles,[4] which correspond to a shock in the hopping particle representation. Throughout this section we use the heat-bath algorithm.

We consider a finite system with stochastic boundary conditions, as described in Section 6. The value of x_{-2L} is chosen with a probability distribution R_θ, where the subscript θ determines the parameters of the measure through formulae (4.10)–(4.12), and x_{2L-1} is chosen with a distribution $Q_{-\theta}$. This choice of boundary condition fixes the average slope of the interface at the boundaries, and the profile must interpolate between these two slopes over the length of the system.

In the infinite system, one is usually interested in a scaling regime where the spatial dimensions are rescaled with the time. In particular, regions of different slopes grow indefinitely with different rates of spreading. This is the basis of the Wulff construction, which determines the profile of the interface from the convex (or concave) envelope of the velocity-slope graph.[2]

For finite lattices, the spreading is limited by the total size, and therefore the final profile will be determined by the slope which spreads the fastest. A roof-shaped profile is defined as a triangular shaped profile with a central region over which the interface slope adapts between the two limiting angles. We deem a such profile to be stable if, as the system size is increased, the tip region remains of size $O(1)$.

The interface profiles are found by averaging configurations over successive Monte Carlo steps, where a Monte Carlo step is defined as one whole odd-even update. The averaging is done at integer times. Two schemes were used for the averaging. The first consisted of calculating the average local slope, $\rho_i = \langle x_i \rangle$ and then summing these quantities, fixing $h_{-2L} = 0$, to find the average interface shape. In the second, the interface is recentered at each time step with respect to a point chosen to move with the peak. There are several possible methods of determining the point

about which to re-center. The simplest is to look for the absolute maximum. This has the disadvantage that there may be, at a given instant, due to fluctuations, more than one candidate, creating a problem of choice, even when the system has an obvious global profile. A possible way to average out fluctuations is to re-center relative to the center of mass. The problem here is that the center of mass moves randomly over a smaller interval than the maximum, and there is no simple relationship connecting the position of the two. In the end we chose a particularly simple method; the higher extremity of the interface profile is chosen, and the level followed until another site at the same height is found. The recentering is then done about the mid-point of this interval. While this method is quite crude, it works well, particularly when the profile has a well defined maximum.

Concave and convex profiles will now be considered separately. The system is taken to be composed of $N=4L$ sites.

7.1. Concave Profiles

In the case of a concave profile ($\theta>0$), there are three distinct possibilities.

1. The interface velocity for angle θ is smaller than for all the angles $\theta' \in]-\theta, \theta[$. Figure 4 shows the average profile, averaged over 10^8 Monte Carlo steps per site for various system sizes, along with the re-centered profiles (averaged over 10^6 Monte Carlo steps). The recentered profiles show that, as the size of the system is increased, the tip of the profile remains of $O(1)$. The slope outside this central region is essentially equal to the boundary value.

Figure 4(b) suggests the interface profile to be essentially of (rounded) triangular shape. If the maximum may be localized anywhere on the lattice with equal probability, the resulting averaged profile would be parabolic, $h=N\tan\theta(x/N-1/2)(x/N+1/2)$, giving a maximum height of $h_{\max}=N/4\tan\theta\approx 0.2$ for $\tan\theta\approx 0.8$, which is the case shown.

Figure 5 shows the average slope or average local density profile in the particle interpretation. A sharply defined roof-shaped profile in the interface picture corresponds to a shock in the particle picture. The averaging process smears out the shock profile. Here, it can clearly be seen that the profile consists of a constant slope, except for a boundary region. From the above considerations, this indicates that the shock has the same probability of being localized at every lattice site (excluding the boundary region).

Figure 6 shows the variation of the maximum height of the rescaled averaged interface as a function of the inverse system size. The results show

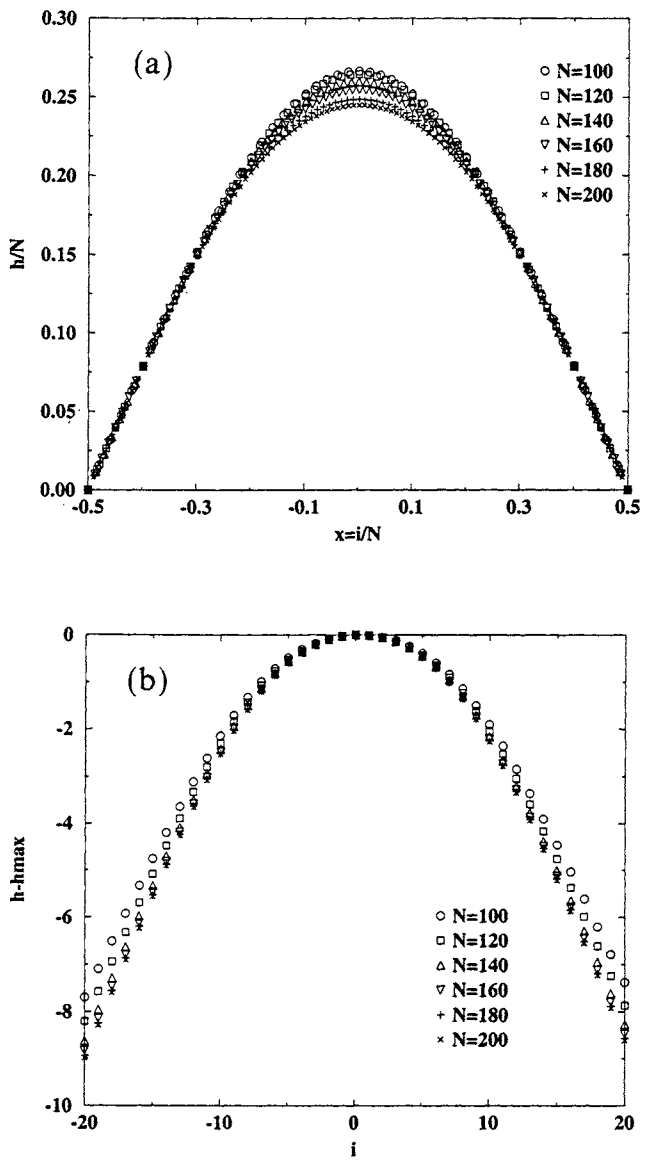

Fig. 4. (a) Interface profile for $E/kT=0.5$, $J/kT=2$ and $y=30(\tan\theta\simeq 0.8)$, averaged with respect to the lattice (only even sites plotted). (b) Interface profile for $E/kT=0.5$, $J/kT=2$ and $y=30$, averaged with recentering (20 sites on both sides of the maximum).

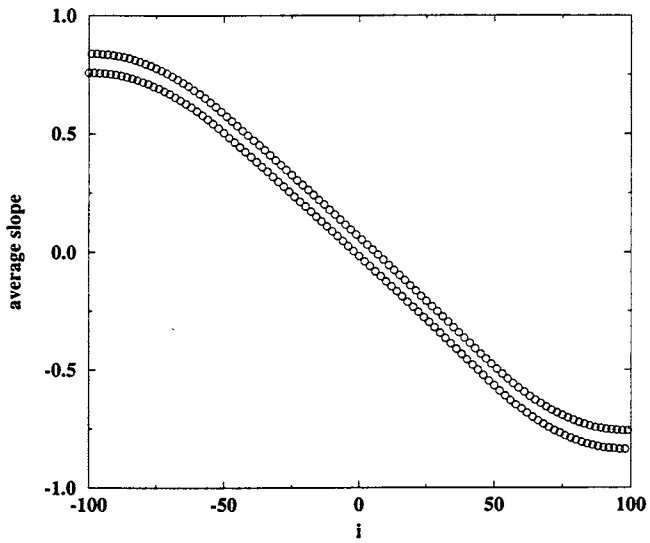

Fig. 5. Average local slope for $E/kT = 0.5$, $J/kT = 2$, $y = 30$ and $N = 200$. The lower set of points corresponds to i even, and the upper i odd.

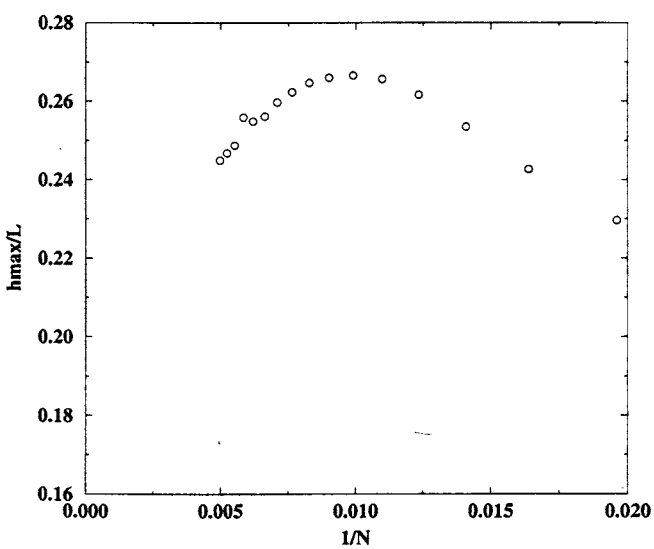

Fig. 6. Variation of the maximal average height plotted as a function of system size ($E/kT = 0.5$, $J/kT = 2$, $y = 30$).

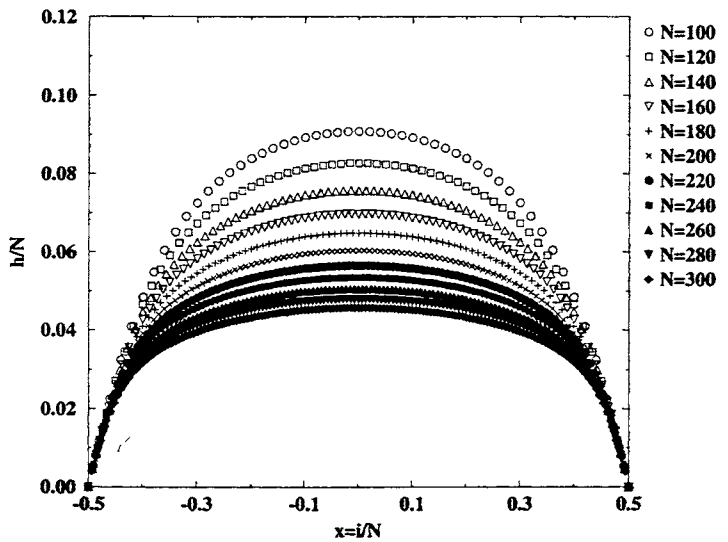

Fig. 7. Interface profile for $E/kT=0.5$, $J/kT=2$ and $y=12(\tan\theta\simeq 0.6)$, averaged with respect to the lattice (only even sites plotted).

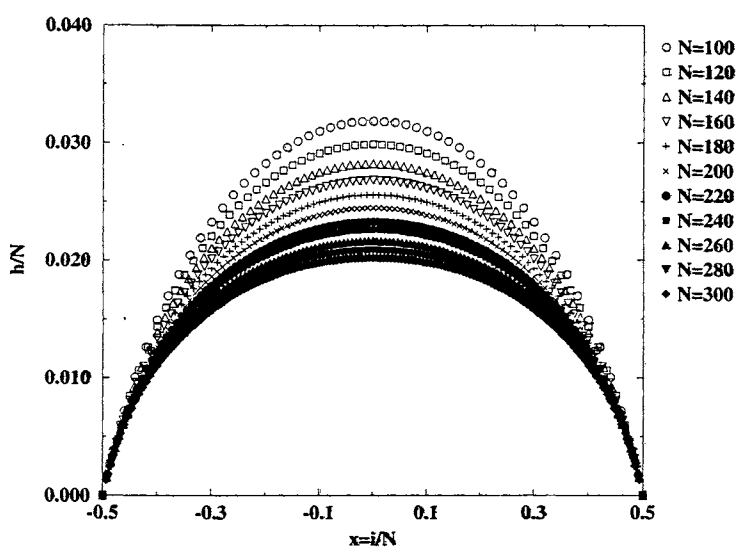

Fig. 8. Interface profile for $E/kT=0.5$, $J/kT=2$ and $y=2.5(\tan\theta\simeq 0.2)$, averaged with respect to the lattice (only even sites plotted).

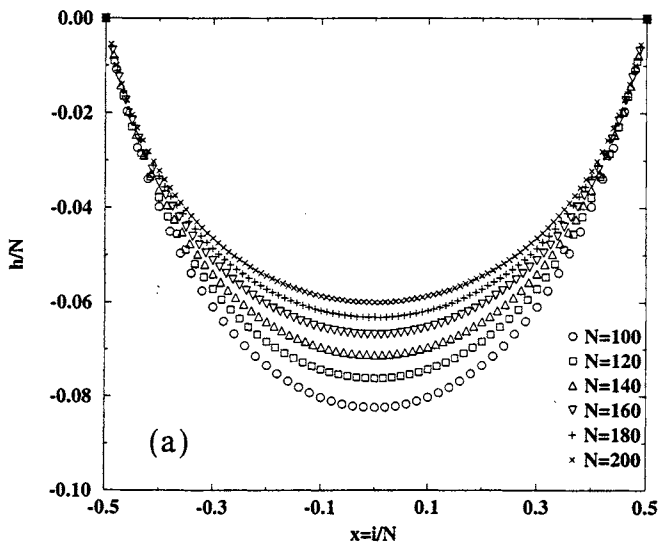

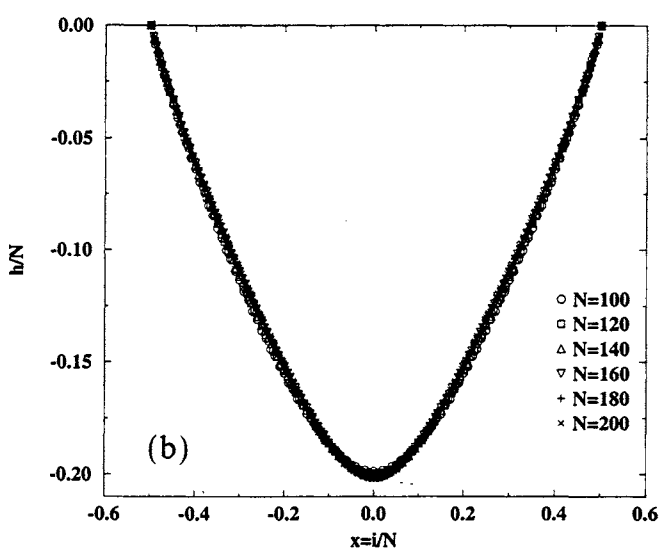

Fig. 9. (a) Average convex interface profiles for $E/kT=0.5$, $J/kT=1$ and $y=1/5(\tan\theta\simeq 0.6)$ (showing only even sites). (b) Average convex interface profiles for $E/kT=0.5$, $J/kT=2$ and $y=1/30(\tan\theta\simeq 0.8)$. (c) Average convex interface profiles for $E/kT=0.5$, $J/kT=2$ and $y=1/2.5(\tan\theta\simeq 0.2)$.

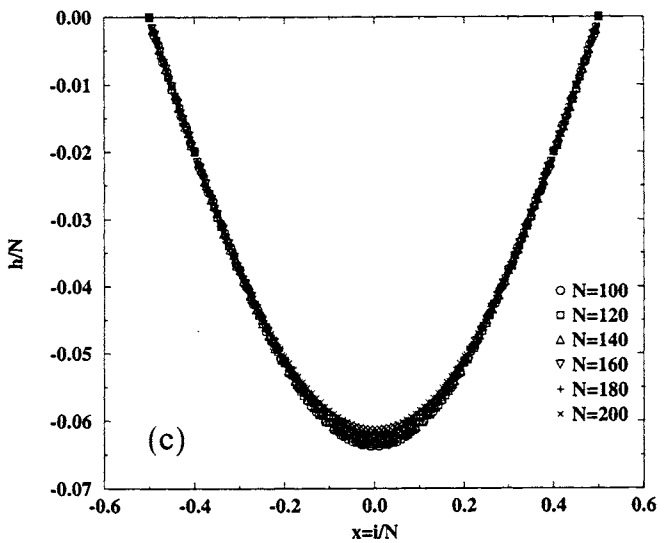

Fig. 9. (*Continued*)

that a limit for $h_{\max}/N$ of about 0.2 is attained for an infinite system size, as predicted above.

These considerations suppose that disturbances due to boundaries can be felt only over a finite distance. This appears indeed to be the case, and a finite size analysis indicates this distance to be of the order of 30–40 lattice sites. Since the interface profile will in practice have a rounded tip with a finite width (here of the order of 30 sites), one can understand this boundary region in terms of the approach of the tip to the edge of the system.

2. The velocity for angle θ is greater than the velocity for an horizontal slope, but the growth velocity is greater than for θ in some range $]\theta', \theta[$, with $\theta' > 0$ (and symmetrically in the range $]-\theta, -\theta'[$). Here the horizontal phase is expected to win. The averaged profiles are flatter, and can clearly be seen to flatten as the system size is increased (Fig. 7). The rescaled height of the interface tends to zero as the system size is increased. The interface must, however, adapt its slope to that fixed at the boundaries. Since the velocity is not monotonic in the slope, we would expect a "kink" to be formed between the angles θ and θ' which have the same velocity. This "kink" will be pushed to the edge of the system, by the emergence of the stable horizontal phase. This may be seen in the profiles shown in Fig. 7; there is a small region close to the boundary where the variation of the slope is important.

Based on this picture, a scaling for the maximum height of the form

$$h_{\max} = a + b(N-c)^d \tag{7.1}$$

may be expected. The value of c corresponds to twice the width of the "kink" localized at the boundary (there being a kink at each end of the lattice). The variation of the $h_{\max}$ with N was fitted using the scaling form (7.1) for both $d=1/2$ and $d=1/3$, both where found to be equally good fits. Unfortunately it would be necessary to go to much larger system sizes in order to determine the right exponent d. However, the boundary region seems in both cases to be of a significant size, consistent with the formation of a boundary kink.

3. The velocity for θ is greater than the velocity for all the angles $\theta' \in]-\theta, \theta[$. Figure 8 shows the average interface profiles. Here too the interface flattens with system size, the flat phase being also the stable phase. The velocity is monotonic in the angle in the range considered. The interfacial slope varies continuously from its value fixed at the boundaries to the horizontal in the middle of the system. This can be seen from the averaged local slopes, which vary more smoothly than in the previous case.

The variation of the height with system size was fitted using (7.1) for $d=1/2$ and $d=1/3$ as above. Again the fits do not discriminate enough to be able to fix the value of the exponent.

7.2 Convex Profiles

For convex profiles ($\theta<0$), slopes which win are those corresponding to the larger growth velocities. Here too there are three generic situations.

1. The velocity decreases monotonically as a function of the slope, the horizontal profile having the greatest growth velocity is the most stable. There is no discontinuity in the allowed slopes, thus there is no structure formed either in the bulk of the system or at the boundaries (Fig. 9(a)).

2. The velocity is maximal at some angle $|\theta_0| < |\theta|$ (Fig. 9(b)).

3. The velocity is smaller for all $|\theta'| < |\theta|$ (Fig. 9(c)).

In the second and third cases, there is a discontinuity in the slopes of the phases which can appear. In the second case the stable phase has a smaller slope than the boundaries, while in the third case, the relatively stable interfaces have slopes $\pm\tan\theta$. A sharp triangular shape is expected in both cases, with a tip of width $O(1)$ formed in the bulk of the system. There is a difference of behavior at the boundaries, which can be seen clearly in Fig. 10. A slope profile similar to the one plotted in Fig. 10(a) has been found already in one-species model by Krug.[14]

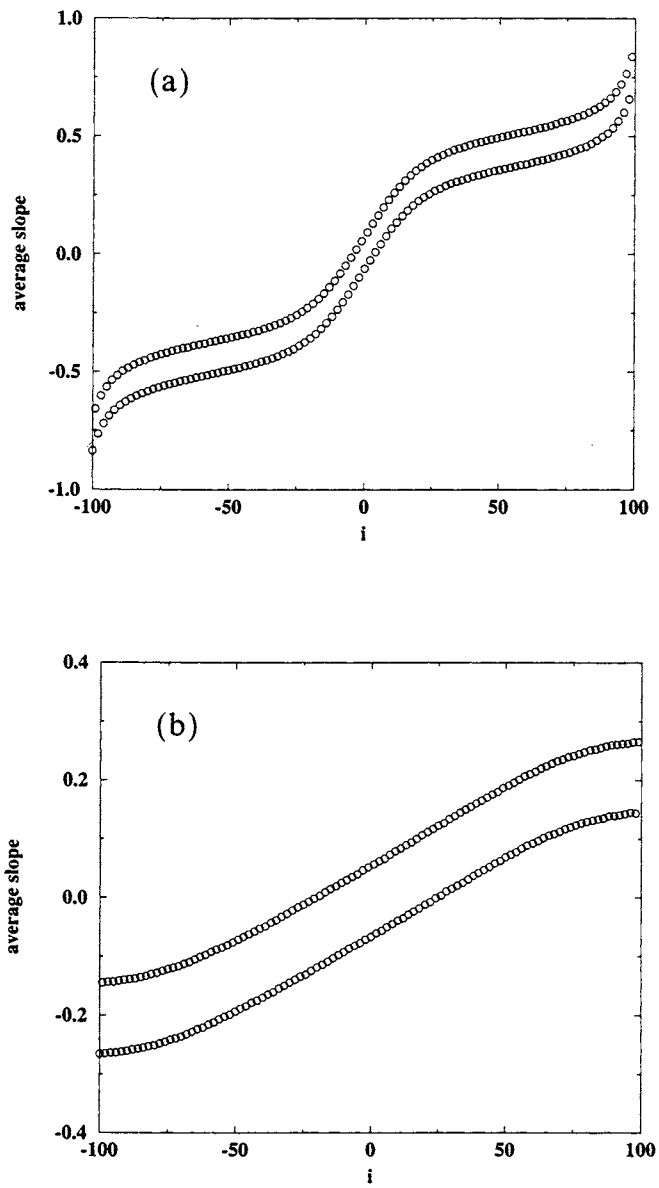

Fig. 10. (a) Average local slope fig $E/kT = 0.5$, $J/kT = 2$ and $y = 1/30$. (b) Average local slope for $E/kT = 0.5$, $J/kT = 2$ and $y = 1/2.5$ The lower set of points corresponds to i even, and the upper i odd.

ACKNOWLEDGMENT

It is a pleasure to thank Lorenzo Bertini, Christian Maes and Mathis Plapp for useful discussions in relation to the present paper.

REFERENCES

1. S. Katz, J. L. Lebowitz and H. Spohn, Nonequilibrium Steady states of stochastic lattice gas models of fast ionic conductors, *J. Stat. Phys.* **34**:497 (1984).
2. J. Krug and H. Spohn, Kinetic Roughening of Growing Surfaces, in "*Solids far from equilibrium*," C. Godrèche ed. (Cambridge University Press, Cambridge, 1991).
3. J. M. J. van Leeuwen and A. Kooiman, The Drift Velocity in the Rubinstein–Duke Model for Electrophoresis, *Physica* **A84**:79 (1992).
4. J. Krug and L-H. Tang, Disoder-induced unbinding in confined geometries, *Phys. Rev.* **E50**:104–115 (1994).
5. T.M. Liggett, A characterization of the invariant measures for an infinite particle system with interactions, I: *Trans. Am. Math. Soc.* **179**:433 (1973); II: *Trans. Am. Math. Soc.* **198**:201 (1974). F. Spitzer, Recurrent random walk on an infinite particle system, *Trans. Am. Math. Soc.* **198**:191 (1974).
6. D. J. Gates, Growth and Decrescence of Two-Dimensional Crystals: A Markov Rate Process, *J. Stat. Phys.* **52**:245–257 (1988).
7. D. J. Gates and M. Westcott, Seven Basic Regimes of Steady Crystal Growth in Two Dimensions, *J. Stat. Phys.* **77**:199–215 (1994).
8. B. Derrida, M. R. Hakim, M. Evans, V. Pasquier, Exact solution of a 1D asymmetric exclusion model using a matrix formulation, *J. Phys.* **A26**:1493 (1993).
9. B. Derrida, S. A. Janowsky, J. L. Lebowitz and E. R. Speer, Microscopic Shock Profiles: Exact Solution of a Non-Equilibrium System, *Europhys. Lett.* **22**:651–656 (1993); Exact Solution of the Totally Asymmetric Simple Exclusion Process: Shock Profiles, *J. Stat. Phys.* **73**:813 (1993).
10. M. R. Evans, D. P. Foster, C. Godrèche and D. Mukamel, Spontaneous symmetry breaking in a one-dimensional driven system, *Phys. Rev. Lett.* **74**:208 (1995); Asymmetric exclusion model with two species: spontaneous symmetry breaking, *J. Stat. Phys.* **80**:69 (1995).
11. H. Hinrichsen, Matrix product ground states for exclusion processes with parallel dynamics, *J. Phys. A* **29**:3659 (1996).
12. N. Rajewski, A. Schadschneider and M. Schreckenberg, The asymmetric exclusion model with sequential update, *J. Phys.* **A29**:L305–L309 (1996).
13. F. Dunlop, M. Plapp, Scaling profiles of a spreading drop from Langevin or Monte Carlo dynamics, pp. 303–308 in "*On Three Levels: Micro-, Meso- and Macro- Approaches in Physics*," Edited by M. Fannes *et al.*, Plenum Press, New-York (1994).
14. J. Krug, Boundary induced phase transitions in driven diffusive systems, *Phys. Rev. Lett.* **67**:1882 (1991).